Bioconjugate Chemistry

Communication

pubs.acs.org/bc

DOTAM Derivatives as Active Cartilage-Targeting Drug Carriers for the Treatment of Osteoarthritis

Hai-Yu Hu,[†,‡,∥] Ngee-Han Lim,[§] Danping Ding-Pfennigdorff,[‡] Joachim Saas,[‡] K. Ulrich Wendt,[‡] Olaf Ritzeler,[‡] Hideaki Nagase,[§] Oliver Plettenburg,[‡] Carsten Schultz,*[,†] and Marc Nazare*[,‡,⊥]

[†]European Molecular Biology Laboratory (EMBL), Interdisciplinary Chemistry Group, Cell Biology and Biophysics Unit, Meyerhofstr. 1, 69117 Heidelberg, Germany

[‡]Sanofi-Aventis Deutschland GmbH, Industriepark Höchst, 65962 Frankfurt, Germany

[§]Kennedy Institute of Rheumatology, University of Oxford, Roosevelt Drive, Headington, Oxford OX3 7FY, United Kingdom

[⊥]Leibniz-Institut für Molekulare Pharmakologie (FMP), Campus Berlin-Buch, Robert-Roessle-Str. 10, 13125 Berlin, Germany

[∥]Department of Chemical Biology, Helmholtz-Zentrum für Infektionsforschung (HZI), Inhoffenstrasse 7, 38124 Braunschweig, Germany

Supporting Information

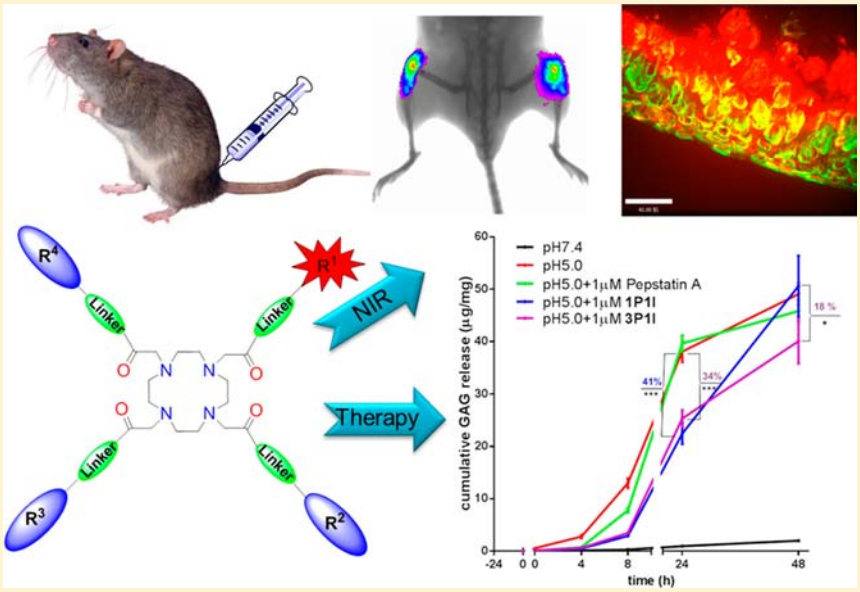

ABSTRACT: Targeted drug-delivery methods are crucial for effective treatment of degenerative joint diseases such as osteoarthritis (OA). Toward this goal, we developed a small multivalent structure as a model drug for the attenuation of cartilage degradation. The DOTAM (1,4,7,10-tetraazacyclododecane-1,4,7,10-tetraacetic acid amide)-based model structure is equipped with the cathepsin D protease inhibitor pepstatin A, a fluorophore, and peptide moieties targeting collagen II. In vivo injection of these soluble probes into the knee joints of mice resulted in 7-day-long local retention, while the drug carrier equipped with a scrambled peptide sequence was washed away within 6−8 h. The model drug conjugate successfully reduced the cathepsin D protease activity as measured by release of GAG peptide. Therefore, these conjugates represent a promising first drug conjugate for the targeted treatment of degenerative joint diseases.

INTRODUCTION

Targeted drug delivery by local administration offers several advantages over systemic administration; particularly, the increased local drug concentration enhances compound exposure and minimizes potential side effects. Such approaches are highly attractive for diseases occurring at clearly localized regions of the body and in tissues that are difficult to penetrate. A prime example is osteoarthritis (OA), a major degenerative joint disease caused by the breakdown of cartilage, in which only one or a very limited number of joints are typically affected.[1] Cartilage

Received: November 29, 2014
Revised: January 26, 2015
Published: January 28, 2015

DOI: 10.1021/bc500557s
Bioconjugate Chem. 2015, 26, 383−388

represents a very challenging tissue for systemic drug delivery, as the presence of highly charged oligosaccharides introduces an effective polar barrier for penetration of lipophilic drug molecules. Another intrinsic challenge results from the fact that low-molecular-weight solutes in the joint compartment experience short residence times between 1 and 2 h due to convective transport and lymphatic uptake.[2] As a result, while local administration via intra-articular (i. art.) injections remains the only effective method to date for delivering drugs into the joint, the rapid clearance from this compartment prevents therapeutic agents from reaching effective concentrations and residence times.[2a−d] Additionally, each i. art. injection bears a considerable risk of serious infection, thus limiting the number and frequency of therapeutic administrations. In attempts to address these issues, drug delivery strategies based on liposomes, nanoparticles, and dendrimers have been reported.[2e,3] A novel, highly attractive approach to overcome these problems is to use an active cartilage-targeting, small-molecule drug carrier platform to deliver the drug to the diseased cartilaginous tissue.[4] Similar strategies employing a targeted drug depot have been based on formulations with polymer carriers.[2d,5] However, small-molecule-based carriers offer significant advantages over polymer-based carriers, including a well-defined size and molecular structure, a more precise and much higher drug loading ratio, a decreased risk of immunogenicity, better shelf stability, and batch-to-batch compositional consistency, thus eliminating the need for strictly regulated manufacturing processes. To the best of our knowledge, no actively targeting, small-molecule drug carrier that increases the residence time in the joint has thus far been reported. Herein, we present the development of a novel DOTAM-based drug-carrier platform as a first small-molecule active cartilage-targeting drug-carrier platform and demonstrate the efficacy of retention in the cartilage of joints both in vitro and in vivo. Furthermore, we validate the ability of this platform to function as an active drug carrier by conjugating the molecule to the cathepsin D inhibitor pepstatin A as a model and showing the increased retention of the conjugate in an ex vivo cartilage model of joint destruction.

Articular cartilage is a highly complex functional tissue comprising of chondrocytes, which are the cells responsible for the generation and homeostasis of cartilage, type II collagen, and proteoglycans, which are composed of glycosaminoglycan (GAG) subunits.[6] To achieve active retention of a small molecule template within cartilage, we reasoned that a multivalent presentation of components that bind either one or both extracellular cartilage constituents would be required. Recently, Hubbell et al. reported pluronic-based nanoparticles functionalized with a specific collagen type II α1-binding peptide sequence WYRGRL which resulted in effective targeting of the nanoparticles to articular cartilage.[4a,7] We reasoned that further addition of cationic moieties like basic amines would simultaneously target the negatively charged sulfated GAGs of the cartilaginous proteoglycans through electrostatic interactions, thereby providing a dual targeting strategy.[8] We selected DOTAM as a tetrapodal template because the molecule is simple to synthesize, highly soluble, nontoxic, and biocompatible, as well as easily functionalized with arm moieties of high conformational flexibility.[9] These features allow variable yet compact multivalent decoration with collagen II-targeting WYRGRL peptides and GAG-targeting amine groups together with the therapeutic agent.

METHODS, RESULTS, AND DISCUSSION

To investigate whether the WYRGRL-DOTAM conjugates display affinity for collagen and cartilage and to optimize the ratio of proteoglycan-to-collagen II binding moieties, we synthesized a series of targeting and control probes labeled with the near-infrared dye Cy 5.5. We used these probes to compare the levels of active targeting of collagen and cartilage in vitro, ex vivo, and in vivo. Scheme 1 shows the synthesis of DOTAM based probes.

Scheme 1. Structures of Cy5.5 Labeled Cartilage Targeting/Control Probes and Inhibitors and General Synthetic Strategy Exemplified by the Synthesis of the Cartilage Targeting DOTAM Cy5.5 Conjugate 3TP[a]

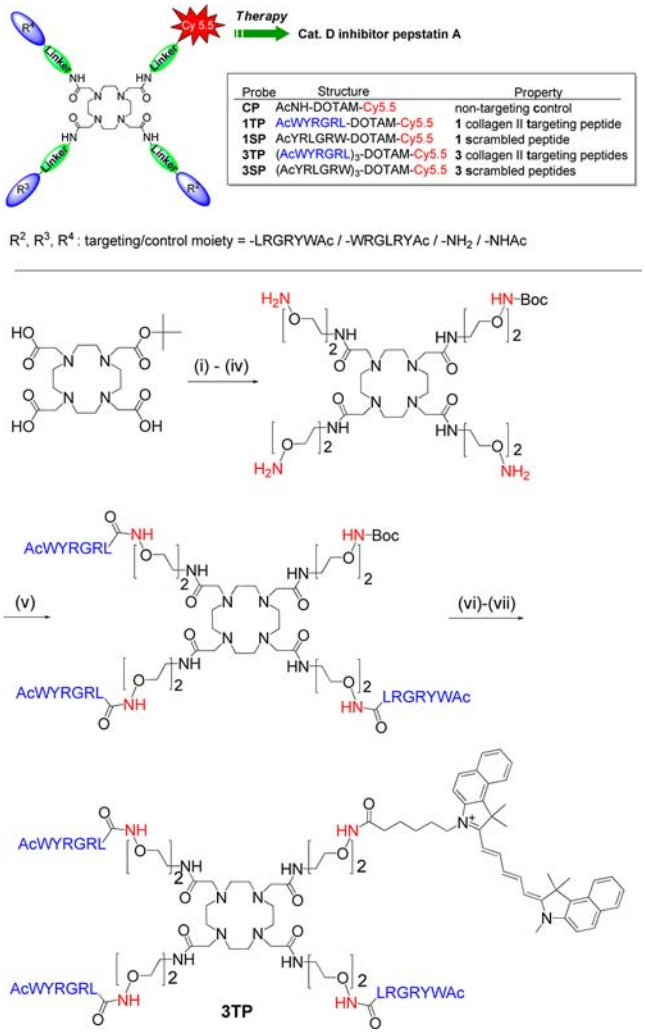

[a]Reactions and conditions: (i) Fmoc-NH-$(PEG)_2$-NH_2, HATU, DIPEA, DMF; (ii) TFA; (iii) Boc-NH-$(PEG)_2$-NH_2, HATU, DIPEA, DMF; (iv) diethylamine/DMF (20%); (v) Ac-WYRGRL−OH, HATU, DIPEA, DMF; (vi) TFA; (vii) Cy 5.5 NHS ester, DIPEA, DMF.

Compounds **1**−**3** derived from DOTA (1,4,7,10-tetraazacyclododecane-1,4,7,10-tetraacetic acid) served as platforms for the synthesis of cartilage-binding and control conjugates and were prepared from triprotected, diprotected, or monoprotected cyclen-derivative compounds **4**−**6** (Supporting Information Scheme S1). The probe **CP** with three capped amine groups was synthesized as a nonbinding control. The terminally acetylated collagen II-binding peptide AcWYRGRL and a scrambled nonbinding peptide AcYRLGRW were synthesized by solid-phase peptide synthesis, and attached to DOTAM template **1**. In a short and efficient sequence of 3 to 4 steps, the probes **1TP** with

DOI: 10.1021/bc500557s
Bioconjugate Chem. 2015, 26, 383−388

one collagen II targeting peptide and two positively charged amine groups, **1SP** with one scrambled peptide and two positively charged amine groups, **3TP** with three collagen II targeting peptides, and **3SP** with three scrambled peptides were synthesized in good yields (see Supporting Information for detailed procedure).

We performed ex vivo binding experiments using pig cartilage explants to evaluate and compare the overall cartilage-targeting affinities and tissue-penetrating characteristics of the five DOTAM-derived compounds. Whole-depth pig articular cartilage blocks were incubated with 1 mL of 5 μM of each probe for 24 h at 37 °C; the blocks were then washed extensively with PBS buffer to remove the nonbinding fraction of the respective probe, followed by imaging using fluorescent microscopy. The probes that entered the cartilage were observed both in the matrix compartment and within the chondrocytes (Figure 1). The intensity of the near-infrared fluorescent signal

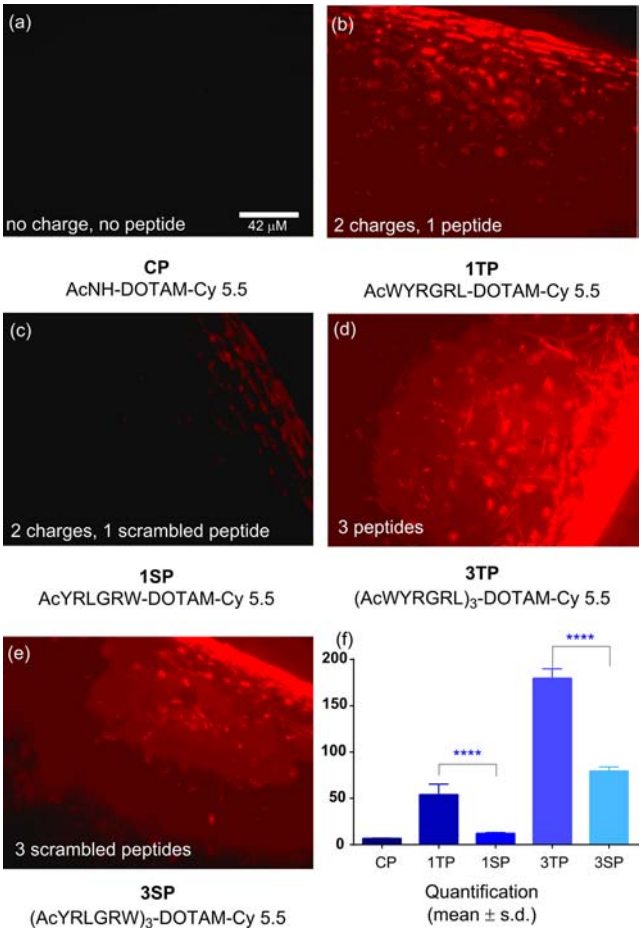

Figure 1. Fluorescent images of pig cartilage explants incubated with (a) nontargeting probe **CP**; (b) probe **1TP** with one collagen II α1-targeted peptide and two basic amine groups; (c) probe **1SP** with one scrambled peptide and two basic amine groups; (d) probe **3TP** with three collagen II α1-targeted peptides; (e) probe **3SP** with three scrambled peptides, all captured at the same settings; (f) quantification of probe content in the pig cartilage. Bars represent mean values ± s.d. (n = 3, **** p < 0.0001).

from Cy5.5 indicated the relevant amount of probe remaining in the cartilage after washing. Interestingly, both the pericellular matrix and the cell nuclei were virtually free from any probe (Supporting Information, Figure S4). Comparison of the targeting probes showed that increasing the number of positive charges and collagen II-targeting peptides attached to the DOTAM template resulted in greater retention of the probe in cartilage. Quantification of probe accumulation by integration of fluorescence intensities in the cartilage revealed a dramatically increased content of targeted probes over their nontargeted controls (Figure 1f). Probe **1TP** (one targeting peptide and two terminal charges) showed an 11.2-fold mean increase over the nontargeting **CP** and a 6.0-fold increase over the nonbinding, scrambled **1SP**, which contained the same net charge but lacked the specific collagen-targeting properties. Probe **3TP** (three targeting peptides) showed a mean 36.6-fold increase over the nontargeting, capped derivative **CP**, a 3.1-fold increase over **1TP**, and a 1.8-fold increase over **3SP** (three scrambled peptides).

The binding capacity of the probes to the knee joint cartilage in mice was evaluated in vivo using optical imaging (OI). Fusion imaging with OI and X-rays allowed colocalization of OI signals with anatomical structures. Intra-articular administration to wild-type mice of the cartilage-targeting probes **1TP** and **3TP** resulted in much longer residence times than observed for the nontargeting control probes **1SP** and **3SP**. As shown in Figure 2a

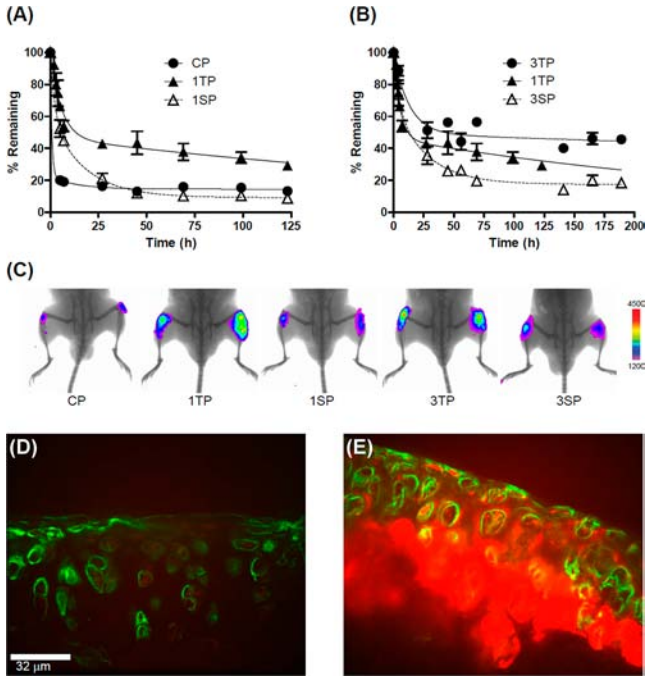

Figure 2. (a,b) In vivo pharmacokinetics of the i. art.-administered DOTAM-based probes in mice knee joints. All data were normalized in individual mice to the intensity at day 0 (100%). The decay in signal was fitted to a two-phase exponential decay model to describe the rapid clearance of unbound probe from the joint and the slower clearance of bound probe from the cartilage (n = 5); (c) representative merged fluorescent and X-ray images showing probe remaining in the knee joints 48 h after i. art. delivery; (d,e) histological studies of nontargeting control probe **CP** (D) and targeting probe **1TP** (E). Merged images of probe distribution (Cy5.5, red) with perlecan (Alexa-488, green) in articular cartilage after 24 h. Images were taken using the same settings.

and b, the probes showed a biphasic clearance pattern: rapid initial clearance of unbound probes from the intra-articular joint space was followed by a slower, second clearance phase of cartilage-bound probe. The probe with the highest retention in cartilage, **3TP**, retained 40% of the initial signal 8 days after injection, whereas the nontargeted **CP** was rapidly cleared to values <20% of the initial signal.[10] The fitted second phase half-lives ($t_{1/2\beta}$) of the targeting probes **1TP** and **3TP** were much

DOI: 10.1021/bc500557s
Bioconjugate Chem. 2015, 26, 383−388

Table 1. Structural Features and in Vitro Cathepsin D Inhibitory Activity (IC_{50} nM values) of DOTAM-Conjugated Compounds Compared to Free Pepstatin A[13]

	Compound				
	Pepstatin A	**CI**	**1P1I**	**3P1I**	**1P3I**
IC_{50}[a]	1.43 ± 0.04	8.55 ± 0.27	6.24 ± 0.40	3.3 ± 0.42	n.d.[b]
R^1		Pepstatin	Pepstatin	Pepstatin	Pepstatin
R^2		H	H	AcWYRGRL	Pepstatin
R^3		H	AcWYRGRL	AcWYRGRL	Pepstatin
R^4		H	H	AcWYRGRL	H

[a]Cathepsin D IC_{50} values were averaged from triplicate measurements and the standard deviation of the positive control was <15% of the mean. [b]Not soluble in buffer.

longer than those observed for the scrambled control probes **1SP** and **3SP**. Figure 2c shows the remaining fluorescence signal for each probe after 48 h, illustrating the increased retention times of **1TP** and **3TP** relative to control probes **CP**, **1SP**, and **3TP**. The probes were also well-tolerated in mice, with no adverse effects observed during the 7 days following administration. These results confirmed that an equal cartilage retention can be achieved in vivo by the AcWYRGRL DOTAM conjugate without using pluronic-based nanoparticles.[4]

The retention and localization of the probes in the mouse cartilaginous compartments was further verified by histological studies (Figure 2d,e). Mice knee joints were harvested 24 h after probe administration and cut into 10 μm sections. A confocal laser microscope was used to visualize the probes by Cy 5.5 fluorescence. Additionally, the extracellular matrix directly surrounding the chondrocyte was visualized by an antibody against perlecan followed by an Alexa-488 secondary antibody. In the **1TP**-treated knee, a strong Cy 5.5 signal was detected specifically in the collagenous areas of the cartilage, whereas noncartilaginous compartments of the joint like the meniscus, synovium, fat tissues, muscles, and bones were free from any Cy 5.5 signal (Supporting Information Figure S3). In the control **CP**-treated knee, only minimal Cy 5.5 fluorescence was detected in the cartilage. When the same settings were used to visualize Cy 5.5 in the **CP**- and **1TP**-treated samples, the **1TP** signal was close to saturation.

The cartilage-targeting results in conjunction with the observed in vivo biocompatibility of the DOTAM-based Cy 5.5 conjugates prompted us to further investigate the suitability of these DOTAM-based derivatives as targeting drug carrier platforms. The loss of proteoglycans, mainly aggrecan, from articular cartilage is one of the hallmarks of the osteoarthritic pathogenesis, which is associated with acidic episodes of the diseased cartilage.[11] When cartilage is maintained at an acidic pH it has been shown that there is a rapid loss of aggrecan from the tissue and it has been suggested that the pH-dependent activation of cathepsin D is responsible for this loss.[12] By inhibition of cathepsin D with pepstatin A, the proteoglycan and cartilage degradation at pH 5.0 is attenuated.[13] Therefore, as a therapeutic model drug we chose pepstatin A, which is particularly challenging due to its inherently low solubility in water. We synthesized a set of DOTAM-based carrier conjugates with one or three pepstatin A ligands. One pepstatin A ligand was conjugated to compound **CI** (zero collagen II α1-targeted peptides and three positively charged amine groups), compound **1P1I** (one collagen II α1-targeted peptide and two positively charged amine groups), and compound **3P1I** (three collagen II α1-targeted peptides). Three pepstatin A ligands were conjugated to compound **1P3I** (one collagen II α1-targeted peptide).

Since most drugs exert very weak or no affinity for the protein target when conjugated to a carrier and therefore require a release mechanism, it was important to determine whether pepstatin A would retain cathepsin D inhibitory activity when covalently linked to the targeting DOTAM conjugate. The inhibitory potency of pepstatin A and four conjugated compounds against cathepsin D was determined in vitro. The conjugation of DOTAM-based carriers caused only minor decreases in inhibitory activity for all three conjugates compared to free pepstatin A. (Detailed procedures are provided in the Supporting Information.) The resulting IC_{50} values are reported in Table 1. In addition, the conjugation of pepstatin A to the polar DOTAM and targeting peptide moieties resulted in a compound with significantly higher solubility than that of free pepstatin A (solubility of pepstatin A = 0.82 mg/mL; **1P1I** > 5.92 mg/mL in phosphate buffer at pH 7.4).

In order to explore the cartilage-targeting affinities of conjugates **1P1I** and **3P1I** relative to free pepstatin A and to determine the effects on osteoarthritis-associated aggrecan degradation, an ex vivo GAG-release experiment with pig articular cartilage explants was carried out.[14] For this study, the explants were preincubated with pepstatin A-DOTAM conjugate **1P1I**, **3P1I**, or free pepstatin A for 24 h and then washed extensively with DMEM buffer to remove unbound inhibitor. Subsequently, the cartilage explants were stimulated by lowering the pH to 5.0 for 48 h. As shown in Figure 3, at 24 h after stimulation, the negative

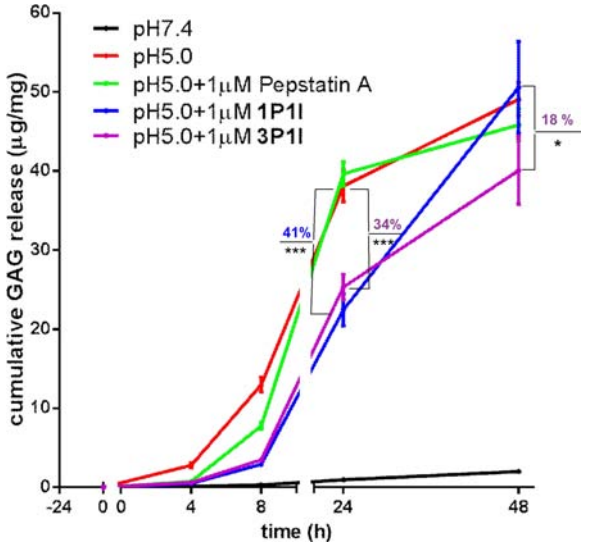

Figure 3. Inhibition of GAG release from cartilage stimulated with pH 5.0 buffer. Cartilage was preincubated with conjugate **1P1I**, **3P1I** or pepstatin A and then stimulated with pH 5.0 buffer. (standard error, $*P < 0.05$; $***P < 0.001$) .

DOI: 10.1021/bc500557s
Bioconjugate Chem. 2015, 26, 383−388

control explants lacking preincubated cathepsin D inhibitor showed an approximately 40-fold increase in GAG release at pH 5.0 over controls (pH 7.4 buffer). Despite the low solubility and therefore suspected partial deposition by precipitation, the free pepstatin A preincubation was not effective in blocking aggrecan breakdown after the washing step, represented by the unaffected level of GAG release. This result indicates that pepstatin A is unable to adhere to the cartilage explants throughout the convective washing step. In contrast, the acid-stimulated GAG release was significantly inhibited by the cartilage-targeting conjugates. Probe **1P1I**, carrying one collagen II targeting moiety, showed 41% inhibition of GAG release at 24 h, but no significant inhibition could be observed at 48 h after stimulation. In contrast, the derivative with the inhibitor conjugated to three targeting peptides (**3P1I**) showed 34% inhibition at 24 h and a still robust 18% at 48 h. The ex vivo experiments clearly demonstrate that the DOTAM-based conjugate enables the inhibitor to localize to and be retained in cartilage tissue much more efficiently than the nonconjugated inhibitor. The impact of collagen-targeting moieties proved to be superior to that of purely charge-dependent effects. This feature is of particular importance, as GAG loss is pronounced even at early to moderate stages of OA, thereby resulting in an overall reduction of negative charges in cartilage layers and reducing the ability to target this component. The active cartilage-targeting properties and the resulting inhibitory effect can thus be prolonged by increasing the targeting peptide number from one to three on the respective adaptor.

CONCLUSION

A general synthetic methodology for the preparation of DOTAM-derived cartilage-targeting carriers has been developed. Ex vivo and in vivo experiments demonstrated that the local exposure and retention time of a DOTAM-conjugated drug can be strongly enhanced by decoration of the DOTAM core with the collagen-binding WYRGRL peptide sequence and basic amines. Conjugation of the core structure to the cathepsin D inhibitor pepstatin A yielded carriers **1P1I** and **3P1I**, which maintained pepstatin A inhibitory activity against cathepsin D in the conjugated state. Notably, in contrast to pepstatin A alone, the conjugates display a very high solubility, underscoring the fact that the described DOTAM platform has the potential to significantly improve physicochemical properties of a parent drug compound. The cartilage-targeting DOTAM-pepstatin A conjugates **1P1I** and **3P1I** were effective over 24 h in the ex vivo GAG release assay in pig cartilage explants, whereas free pepstatin A showed no effect. These findings demonstrate the potential of the DOTAM-based cartilage-targeting drug carrier system to significantly prolong the drug's duration of action by extending the residence time in articular cartilage. Thus, this DOTAM-based carrier can be conveniently conjugated to drugs to allow addition and fine-tuning of biochemical properties. The ability of these conjugates to target, be retained, and act on cartilage is particularly significant for advancing OA treatment.

ASSOCIATED CONTENT

Supporting Information

Supplemental figures, synthetic schemes, experimental procedures, characterization of all new compounds, immunofluorescence staining for Perlecan, experimental procedures of binding affinities of Cy 5.5 labeled compounds and inhibition studies of DOTAM conjugates. This material is available free of charge via the Internet at http://pubs.acs.org.

AUTHOR INFORMATION

Corresponding Authors

*E-mail: schultz@embl.de.

*E-mail: nazare@fmp-berlin.de.

Author Contributions

All authors have given approval to the final version of the manuscript. Hai-Yu Hu and Ngee-Han Lim contributed equally.

Notes

The authors declare no competing financial interest.

ACKNOWLEDGMENTS

All authors acknowledge funding by LIVIMODE, a collaborative project funded by the EU FP7. We thank Dr. Marcie B. Jaffee for critical comments and helpful discussions.

REFERENCES

(1) Lawrence, R. C., Helmick, C. G., Arnett, F. C., Deyo, R. A., Felson, D. T., Giannini, E. H., Heyse, S. P., Hirsch, R., Hochberg, M. C., Hunder, G. G., Liang, M. H., Pillemer, S. R., Steen, V. D., and Wolfe, F. (1998) Estimates of the prevalence of arthritis and selected musculoskeletal disorders in the United States. *Arthritis Rheum. 41*, 778−799.

(2) (a) Aly, N. M. (2008) Intra-articular drug delivery: a fast growing approach. *Recent Pat. Drug Delivery Formul. 2*, 231−237. (b) Butoescu, N., Jordan, O., and Doelker, E. (2009) Intra-articular drug delivery systems for the treatment of rheumatic diseases: a review of the factors influencing their performance. *Eur. J. Pharm. Biopharm. 73*, 205−218. (c) Chevalier, X. (2010) Intraarticular treatments for osteoarthritis: new perspectives. *Curr. Drug Targets 11*, 546−560. (d) Gerwin, N., Hops, C., and Lucke, A. (2006) Intraarticular drug delivery in osteoarthritis. *Adv. Drug Delivery Rev. 58*, 226−242. (e) Larsen, C., Ostergaard, J., Larsen, S. W., Jensen, H., Jacobsen, S., Lindegaard, C., and Andersen, P. H. (2008) Intra-articular depot formulation principles: role in the management of postoperative pain and arthritic disorders. *J. Pharm. Sci. 97*, 4622−4654. (f) Zhang, Z., and Huang, G. (2012) Micro- and nano-carrier mediated intra-articular drug delivery systems for the treatment of osteoarthritis. *J. Nanotechnol. 2012*, 1−11.

(3) (a) Evans, C. H., Kraus, V. B., and Setton, L. A. (2014) Progress in intra-articular therapy. *Nat. Rev. Rheumatol. 10*, 11−22. (b) Haag, R., and Kratz, F. (2006) Polymer therapeutics: concepts and applications. *Angew. Chem., Int. Ed. 45*, 1198−1215. (c) Byrne, J. D., Betancourt, T., and Brannon-Peppas, L. (2008) Active targeting schemes for nanoparticle systems in cancer therapeutics. *Adv. Drug Delivery Rev. 60*, 1615−1626. (d) Singh, R., and Lillard, J. W., Jr. (2009) Nanoparticle-based targeted drug delivery. *Exp. Mol. Pathol. 86*, 215−223. (e) Röglin, L., Lempens, E. H. M., and Meijer, E. W. (2011) A synthetic "tour de force": well-defined multivalent and multimodal dendritic structures for biomedical applications. *Angew. Chem., Int. Ed. 50*, 102−112. (f) Khandare, J., Calderon, M., Dagia, N. M., and Haag, R. (2012) Multifunctional dendritic polymers in nanomedicine: opportunities and challenges. *Chem. Soc. Rev. 41*, 2824−2848.

(4) (a) Rothenfluh, D. A., Bermudez, H., O'Neil, C. P., and Hubbell, J. A. (2008) Biofunctional polymer nanoparticles for intra-articular targeting and retention in cartilage. *Nat. Mater. 7*, 248−254. (b) Setton, L. (2008) Polymer therapeutics: reservoir drugs. *Nat. Mater. 7*, 172−174.

(5) Parthiban, C. P., Jeroen, C. H. L., Pieter, J. D., Marcel, K., and Janine, N. P. (2012) Nanomaterials for the local and targeted delivery of osteoarthritis drugs. *J. Nanomater. 2012*, 1−13.

(6) Chen, F. H., Rousche, K. T., and Tuan, R. S. (2006) Technology Insight: adult stem cells in cartilage regeneration and tissue engineering. *Nat. Clin. Pract. Rheum. 2*, 373−382.

(7) Cabanas-Danés, J., Nicosia, C., Landman, E., Karperien, M., Huskens, J., and Jonkheijm, P. (2013) A fluorogenic monolayer to detect the co-immobilization of peptides that combine cartilage targeting and regeneration. *J. Mater. Chem. B 1*, 1903−1908.

DOI: 10.1021/bc500557s
Bioconjugate Chem. 2015, 26, 383−388

(8) Joshi, N. S., Bansal, P. N., Stewart, R. C., Snyder, B. D., and Grinstaff, M. W. (2009) Effect of contrast agent charge on visualization of articular cartilage using computed tomography: exploiting electrostatic interactions for improved sensitivity. *J. Am. Chem. Soc. 131*, 13234−13235.
(9) De León-Rodríguez, L. M., and Kovacs, Z. (2008) The synthesis and chelation chemistry of DOTA−peptide conjugates. *Bioconjugate Chem. 19*, 391−402.
(10) We attribute the residual fluorenscence effect due to unspecific passive deposition at adjacent non-cartilageneous compartments after i. art. application in mice, since we could detect only minimal Cy5.5 fluorescense in the subsequent histological examination of these knees using cryo-section and confocal laser microscopy. For similar behavior and observation see: Kara, M. H., Erin, L. C., and Bradley, D. S. (2013) In vivo imaging of bone using a deep-red fluorescent molecular probe bearing multiple iminodiacetate group. *Mol. Pharmaceutics 10*, 4263−4271.
(11) Troeberg, L., and Nagase, H. (2012) Proteases involved in cartilage matrix degradation in osteoarthritis. *Biochim. Biophys. Acta 1824*, 133−145.
(12) (a) McAdoo, M. H., Dannenberg, A. M., Hayes, C. J., James, S. P., and Sanner, J. H. (1973) Inhibition of the Cathepsin D-type proteinase of macrophages by pepstatin, a specific pepsin inhibitor, and other substances. *Infect. Immun. 7*, 655−665. (b) Konttinen, Y. T., Mandelin, J., Li, T. F., Salo, J., Lassus, J., Liljeström, M., Hukkanen, M., Takagi, M., Virtanen, I., and Santavirta, S. (2002) Acidic cysteine endoproteinase cathepsin K in the degeneration of the superficial articular hyaline cartilage in osteoarthritis. *Arthritis Rheum. 46*, 953−960.
(13) Dingle, J. T., Barrett, A. J., Poole, A. R., and Stovin, P. (1972) Inhibition by pepstatin of human cartilage degradation. *Biochem. J. 127*, 443−444.
(14) (a) Handley, C. J., Tuck Mok, M., Ilic, M. Z., Adcocks, C., Buttle, D. J., and Robinson, H. C. (2001) Cathepsin D cleaves aggrecan at unique sites within the interglobular domain and chondroitin sulfate attachment regions that are also cleaved when cartilage is maintained at acid pH. *Matrix Biol. 20*, 543−553. (b) Lim, N. H., Kashiwagi, M., Visse, R., Jones, J., Enghild, J. J., Brew, K., and Nagase, H. (2010) Reactive-site mutants of N-TIMP-3 that selectively inhibit ADAMTS-4 and ADAMTS-5: biological and structural implications. *Biochem. J. 431*, 113−122.

DOI: 10.1021/bc500557s
Bioconjugate Chem. 2015, 26, 383−388